Reversible interconversion between a nitrido complex of Os(VI) and an ammino complex of osmium(II)

ARTICLE *in* JOURNAL OF THE AMERICAN CHEMICAL SOCIETY · JULY 1990

Impact Factor: 12.11 · DOI: 10.1021/ja00170a014

5 AUTHORS, INCLUDING:

Mohammed Bakir
The University of the West Indies at Mona

103 PUBLICATIONS **1,003** CITATIONS

SEE PROFILE

Reversible Interconversion between a Nitrido Complex of Os(VI) and an Ammino Complex of Osmium(II)

David W. Pipes, Mohammed Bakir, S. E. Vitols, Derek J. Hodgson,‡ and Thomas J. Meyer*

Contribution from the Department of Chemistry, University of North Carolina, Chapel Hill, North Carolina 27599-3290, and Chemistry Department, University of Wyoming, Laramie, Wyoming 82071-3838. *Received September 1, 1989*

Abstract: The reaction between $[N(n\text{-}Bu)_4][Os(N)(X)_4]$ (X = Cl, Br) and 2,2′:6′,2″-terpyridine (tpy) in acetone under reflux gave the salts $[Os(N)(typ)(X)_2]X$. The X-ray crystal structure of $[Os(N)(tpy)(Cl)_2]Cl$ showed that the chloride ligands occupy mutually trans axial positions relative to the nitrido ligand. The effects of multiple bonding in the Os–N bond appear in the short Os–N bond length of 1.663 (5) Å, in the bending of the ligating atoms in the cis positions away from the Os–N axis, and in the elongation of the trans N atom of the bound tpy by 0.08 Å. Electrochemical or chemical reduction of the nitrido complex in acidic aqueous solution gave the corresponding ammino complex of Os(II), $[Os(NH_3)(tpy)(Cl)_2]$, which, following oxidation by air, was isolated as the corresponding PF_6 salt of Os(III). The Os(II)–ammine complex could be reoxidized to the nitrido complex either chemically or electrochemically. Reduction potentials were measured or estimated at pH = 3 for the intermediate Os(VI/V), Os(V/IV), Os(IV/III), and Os(III/II) couples. From those measurements, it was shown that the Os(V) intermediate, $[Os^{V}(N)(tpy)(Cl)_2]$, is both a powerful oxidant and a strong reductant, highly unstable with respect to disproportionation into Os(VI) and Os(IV). Oxidation state IV as $[Os^{IV}(NH_3)(tpy)(Cl)_2]^{2+}$ is unstable with respect to disproportionation into Os(VI) and Os(III).

Key steps in the catalytic or stoichiometric reduction of nitrite to ammonia by transition-metal complexes include the initial binding of nitrite, acid–base interconversion to nitrosyl,[1] and the reduction of nitrosyl to ammonia.[2] In polypyridyl complexes of Ru and Os such as $[M(NO)(tpy)(bpy)]^{3+}$ (tpy is 2,2′:6,2″-terpyridine; bpy is 2,2′-bipyridine; M = Ru or Os), it has been found that the interconversion between nitrosyl and ammonia can be made reversible in aqueous solution.[2a,b] Reaction schemes have

$$[Ru^{II}(NO)(tpy)(bpy)]^{3+} \underset{-6e^-,\,-5H^+,\,+H_2O}{\overset{+6e^-,\,+5H^+,\,-H_2O}{\rightleftharpoons}} [Ru^{II}(NH_3)(tpy)(bpy)]^{2+} \quad (1)$$

been proposed in which a series of concomitant electron/proton transfers occur coupled with hydration–dehydration to give intermediates such as $[M^{VI}(N)(tpy)(bpy)]^{3+}$, $[M(NHO)(tpy)(bpy)]^{2+}$, $[M(NH_2O)(tpy)(bpy)]^{2+}$, $[M^{V}(N)(tpy)(bpy)]^{2+}$, or $[M^{IV}(NH)(tpy)(bpy)]^{2+}$.[2-4] Although none of these intermediates has been isolated and properly characterized, related examples are known in different coordination environments. This is particularly true of nitrido complexes of Os(VI) where several examples have been described.[5-9]

There is an interesting correspondence between certain of these intermediates. For example, an electron count shows that the Os(VI) nitrido complex, $[Os(N)(bpy)Cl_3]$, is equivalent in electron content to the twice-reduced form of $[Os(NO)(tpy)(bpy)]^{3+}$.[2a,b]

$$[Os^{II}(NO)(tpy)(bpy)]^{3+} + 2e^- \rightarrow [Os(NO)(tpy)(bpy)]^{+}$$

The nitrosyl and nitrido forms are interrelated by a hydration–dehydration reaction.

$$[Os^{VI}(N)(bpy)(Cl)_3] + 2OH^- \rightleftharpoons [Os(NO)(bpy)(Cl)_3]^{2-} + H_2O$$

The possible existence of hydrated and dehydrated forms having equivalent electron contents and the correspondence between the reduced nitrosyl and the nitrido complexes raise some significant issues. One is how relatively minor changes in the ligands, in this case the replacement of three Cl^- by tpy, can play such a significant role in dictating which of the possible forms will be stable in intermediate oxidation states. Another is how the chemistries of the different intermediates are interrelated.

We report here the preparation, structure, and redox properties of *trans*-$[Os^{VI}(N)(tpy)(Cl)_2]^{+}$. The synthetic chemistry of polypyridyl–nitrido complexes of Os(VI) has been developed in considerable detail in the dissertation of Ware.[9] There, a series of complexes was prepared and a thermally induced coupling chemistry was described based on the appearance of Os(III) and N_2 as products. Our interests were in uncovering the interconversion chemistry between nitrosyl, nitrido, and ammino forms, the implications that such reactions might have for the reduction of nitrite to ammonia, and the effect on the underlying chemistry of the exchange of halide ions for pyridyl ligands in the coordination sphere of the metal ion.

Experimental Section

Materials. The chemicals 2,2′-bipyridine, osmium tetraoxide (>99%), 2,2′:6′,2″-terpyridine, and $^{15}NH_4Cl$ (>99%) were obtained from Aldrich Chemical Co. All other chemicals were of reagent grade and used without further purification.

Measurements. Electronic absorption spectra were recorded on Beckman 2000, Cary 14, or HP 8451A UV–visible spectrophotometers. Solution ^1H NMR spectra were obtained in CD_3CN and recorded on a Brüker 250-MHz Fourier transform spectrometer by using TMS as a reference. Electrochemical measurements were made in solutions of acetonitrile with 0.1 M tetra-*n*-butylammonium hexafluorophosphate (TBAH) as the supporting electrolyte or in aqueous solutions of varying ionic compositions. A platinum bead working electrode was used for measurements in CH_3CN solutions and a glassy carbon working electrode was used for measurements in aqueous solutions. All potentials were referenced to the saturated sodium chloride calomel electrode (SSCE)

* Address correspondence to this author at the University of North Carolina.
‡ University of Wyoming.

(1) (a) Feltham, R. P. *Top. Stereochem.* **1981**, *12*, 155. (b) McCleverty, J. A. *Chem. Rev.* **1979**, *79*, 53.
(2) (a) Murphy, W. R., Jr.; Takeuchi, K.; Meyer, T. J. *J. Am. Chem. Soc.* **1982**, *104*, 5817. (b) Barley, M. H.; Takeuchi, K.; Murphy, W. R., Jr.; Meyer, T. J. *J. Chem. Soc., Chem. Commun.* **1985**, 507. (c) Murphy, W. R., Jr.; Takeuchi, K.; Barley, M. H.; Meyer, T. J. *Inorg. Chem.* **1986**, *25*, 1041. (d) Rhodes, M.; Meyer, T. J. *Inorg. Chem.* **1988**, *27*, 4772.
(3) Rhodes, M.; Meyer, T. J. Submitted.
(4) Thompson, M. S.; Meyer, T. J. *J. Am. Chem. Soc.* **1981**, *103*, 5577.
(5) Nugent, W. A.; Mayer, J. M. *Metal Ligand Multiple Bonds*; John Wiley & Sons: New York, 1988.
(6) Griffith, W. P. *Coord. Chem. Rev.* **1972**, *8*, 369.
(7) (a) Belmonte, P. A.; Zang-Yuan, O. *J. Am. Chem. Soc.* **1984**, *106*, 7493. (b) Griffith, W. P.; McManus, N. T.; White, A. D. *J. Chem. Soc., Dalton Trans.* **1986**, *5*, 1035. (c) Griffith, W. P.; Wright, M. *Trans. Met. Chem.* **1982**, *7*, 53. (d) Griffith, W. P.; Pawson, D. *J. Chem. Soc., Dalton Trans.* **1973**, 1315. (e) Sen, D.; Ta, N. C. *Indian J. Chem.* **1978**, *16A*, 859.
(8) Buhr, J. D.; Taube, H. *Inorg. Chem.* **1979**, *18*, 2208.
(9) Ware, D. Ph.D. Dissertation, Stanford University, 1986.

0002-7863/90/1512-5507$02.50/0

Table I. Crystallographic and Data Collection Parameters

formula: $OsC_{15}H_{11}N_4Cl_3$	D_o = 2.25 (3) g cm^{-3}
a = 8.767 (2) Å	Z = 4
b = 8.930 (3) Å	D_c = 2.222
c = 21.103 (4) Å	space group: $P2_1/n$
β = 100.23 (2)°	μ = 88.3 cm^{-1}
V = 1626 (1) Å^3	data range 2° ≤ θ(Mo) ≤ 27°
No. ($>3\sigma$) = 2521	max transmission: 99.98%
T = 20 °C	min transmission: 75.91%
radiation: Mo Kα	av transmission: 88.75%
data collected: $+h, +k, +l$	

at room temperature and are uncorrected for junction potentials. In controlled-potential electrolysis experiments, H-shaped cells with oxidative and reductive compartments separated by a sintered glass disk were used; the working electrode was reticulated vitreous carbon. Voltammetric experiments were performed with the use of a PAR 173 Galvanostat/Potentiostat in conjunction with a home-built supercycle,[10] and a SOLTEC VP-6414S X-Y recorder. A PAR 179 digital coulometer was used in conjunction with a PAR 173 galvanostat/potentiostat for coulometry experiments. Infrared spectra were recorded as KBr pellets on a Nicolet 20DX FTIR spectrometer.

Preparations. The following complexes were prepared by using literature procedures: K[Os(N)(O)$_3$],[11a] K[Os(^{15}N)(O)$_3$], [N(n-Bu)$_4$][Os(N)(Cl)$_4$],[11b] [N(n-Bu)$_4$][Os(^{15}N)(Cl)$_4$],[11b] [N(n-Bu)$_4$][Os(N)(Br)$_4$].[11b]

[Os(N)(tpy)(Cl)$_2$]Cl. A slightly modified procedure from that described by Ware[9] was used. A mixture of [N(n-Bu)$_4$][Os(N)(Cl)$_4$] (200 mg, 0.33 mmol) and tpy (110 mg, 0.48 mmol) was stirred in refluxing acetone (10 mL) for 48 h. The resulting dark purple solid was filtered off, washed with acetone, hexanes, and ether, and dried: yield 130 mg (72%). Anal. Calcd for $C_{15}H_{11}Cl_3N_4Os$: C, 33.13; H, 2.04; Cl, 19.55; N, 10.30. Found: C, 33.12; H, 2.22; Cl, 19.22; N, 10.25. Single crystals of [Os(N)(tpy)(Cl)$_2$]Cl were grown as follows. The salt [N(n-Bu)$_4$][Os(N)(Cl)$_4$] (100 mg, 0.16 mmol) was dissolved in 5 mL of acetone with tpy (44.9 mg, 0.19 mmol). The solution was allowed to stand at room temperature for 24 h. The fine needlelike crystals were filtered off and washed with acetone.

[Os(N)(tpy)(Cl)$_2$]PF$_6$. [Os(N)(tpy)(Cl)$_2$]Cl (50 mg, 0.09 mmol) was suspended in CH_3CN (10 mL) and HPF_6 was added dropwise until all of the chloride salt was dissolved. The reaction mixture was stirred at room temperature for 5 min and diethyl ether was added to precipitate the pink hexafluorophosphate salt. The resulting product was recrystallized twice from CH_3CN/ether, filtered, and dried: yield 30 mg (51%). The product was characterized as [Os(N)(tpy)(Cl)$_2$](PF$_6$) from a comparison between its electrochemical and spectroscopic properties and those of the Cl$^-$ salt.

[Os(N)(tpy)(Br)$_2$]Br. The identical procedure was used as for the preparation of [Os(N)(tpy)(Cl)$_2$]Cl except that [N(n-Bu)$_4$][Os(N)(Br)$_4$] was used as the starting material. Anal. Calcd for $C_{15}H_{11}Br_3N_4Os$: C, 26.60; H, 1.64; N, 8.27. Found: C, 26.77; H, 1.68; N, 8.21.

[Os(^{15}N)(tpy)(Cl)$_2$]Cl. The same procedure was used as for the preparation of [Os(N)(tpy)(Cl)$_2$]Cl except that [N(n-Bu)$_4$][Os(^{15}N)(Cl)$_4$] was used as the starting material.

[Os(^{15}N)(bpy)(Cl)$_3$]. The same procedure was used as for the preparation of [Os(^{15}N)(tpy)(Cl)$_2$] except that 1.1 equiv of 2,2′-bipyridine were added. The preparation of the complex of normal isotopic composition has also been described by Ware.[9]

[Os(NH$_3$)(tpy)(Cl)$_2$](PF$_6$). [Os(N)(tpy)(Cl)$_2$]Cl (50 mg, 0.089 mmol) was reduced at a potential of −0.5 V at a vitreous carbon electrode in 3 M HCl. The electrolysis was complete after 33 C when n = 4. The resulting brown solution was reduced in volume to ~2 mL and KPF_6 (200 mg) was added. The reaction mixture was allowed to stand in an ice bath for 30 min. The resulting brown solid was filtered off, washed with cold water and ether, and dried: yield 20 mg (33%). Anal. Calcd for $C_{15}H_{14}Cl_2F_6NOsP$: C, 27.44; H, 2.15; Cl, 10.80; N, 8.54. Found: C, 27.84; H, 2.51; Cl, 10.34; N, 8.36.

Collection and Reduction of the X-ray Data. A magenta-colored, parallelpiped-shaped crystal of [Os(N)(tpy)(Cl)$_2$]Cl was used for data collection on an Enraf-Nonius CAD-4 diffractometer by using Mo Kα radiation and a graphite monochromator. Cell parameters and other crystallographic information are given in Table I along with additional details concerning the collection of data.

(10) Woodward, W. S.; Rocklin, R. D.; Murray, R. W. *Chem., Biomed. Environ. Instrum.* **1979**, *9*, 95.

(11) (a) Clifford, A. F.; Kobayashi, C. S. *Inorg. Synth.* **1960**, *6*, 204. (b) Cowman, C. D.; Trogler, W. C.; Mann, K. R.; Gray, H. B. *Inorg. Chem.* **1976**, *15*, 1749.

Table II. Atomic Positional Parameters for [Os(N)(tpy)(Cl)$_2$]Cl Based on the Labeling Scheme in Figure 1

atom	x	y	z
Os	0.11239 (3)	0.14487 (3)	0.14910 (1)
Cl(1)	0.1834 (2)	0.1045 (2)	0.04830 (8)
Cl(2)	0.0413 (2)	0.2505 (2)	0.24128 (8)
Cl(3)	0.3621 (2)	0.2663 (2)	0.89009 (9)
N(1)	0.1118 (7)	−0.0332 (6)	0.1720 (3)
N(2)	−0.1132 (6)	0.1864 (5)	0.1035 (2)
N(2′)	0.1142 (5)	0.3769 (5)	0.1200 (2)
N(2″)	0.3376 (6)	0.2192 (6)	0.1832 (2)
C(1)	−0.1485 (7)	0.3301 (6)	0.0818 (3)
C(3)	−0.2264 (8)	0.0850 (7)	0.0958 (3)
C(4)	−0.3762 (8)	0.1174 (8)	0.0664 (3)
C(5)	−0.4124 (8)	0.2580 (8)	0.0449 (3)
C(6)	−0.2978 (7)	0.3658 (7)	0.0529 (3)
C(1′)	−0.0185 (7)	0.4370 (7)	0.0904 (3)
C(3′)	0.2490 (7)	0.4519 (7)	0.1314 (3)
C(4′)	0.2518 (7)	0.5995 (6)	0.1118 (3)
C(5′)	0.1169 (8)	0.6654 (6)	0.0820 (3)
C(6′)	−0.0202 (8)	0.5872 (7)	0.0708 (3)
C(1″)	0.3757 (7)	0.3631 (7)	0.1679 (3)
C(3″)	0.4439 (8)	0.1372 (8)	0.2208 (3)
C(4″)	0.5881 (8)	0.1896 (8)	0.2450 (4)
C(5″)	0.6274 (7)	0.3301 (7)	0.2288 (3)
C(6″)	0.5211 (7)	0.4167 (7)	0.1898 (3)

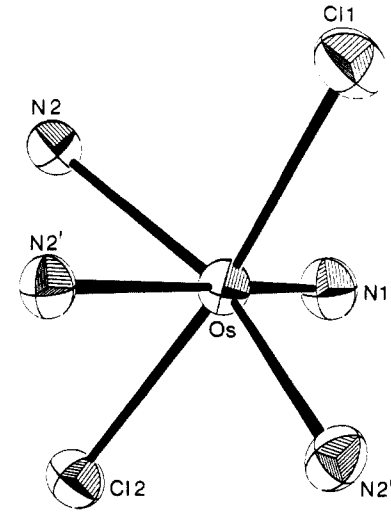

Figure 1. View of the coordination geometry around Os(VI) in the [Os(N)(tpy)(Cl)$_2$]$^+$ cation. Atom N(1) is the nitrido ligand, while atoms N(2), N(2′), and N(2″) are the nitrogen atoms of the tpy ligand.

Solution and Refinement of the Structure. The location of the osmium atom was determined unambiguously from a Patterson map, and the remaining non-hydrogen atoms were located in subsequent difference Fourier maps. Isotropic refinement of the 23 non-hydrogen atoms, by using a small subset of the data (774 reflections), converged to values of the conventional agreement factors, $R_1 = S||F_o| - |F_c||/S|F_o|$ and $R_2 = [S(|F_o| - |F_c|)^2/S|F_o|^2]^{1/2}$ of 0.034 and 0.0367, respectively. Anisotropic refinement, by using the full data set, reduced these values to 0.031 and 0.034, respectively. The location of all 11 hydrogen atoms was deduced from a difference Fourier synthesis, and these atomic positions were refined isotropically in subsequent least-squares iterations. The final cycle of the least-squares analysis involved 2521 observations and 252 variables and converged to values of R_1 and R_2 of 0.028 and 0.027, respectively. A final difference Fourier map was featureless with no peak higher than 0.5 e·Å^{-3}. The final positional parameters, along with their standard deviations as estimates from the inverse matrix, are presented in Table II. Tables of hydrogen atom parameters, anisotropic thermal parameters, and observed/calculated structure amplitudes are available as supplementary material.

Results

Description of the Structure. The structure of the salt [Os(N)(tpy)(Cl)$_2$]Cl consists of monomeric *trans*-[Os(N)(tpy)(Cl)$_2$]$^+$ cations and chloride anions that are well separated from each other. The coordination around the metal ion is depicted in Figure 1,

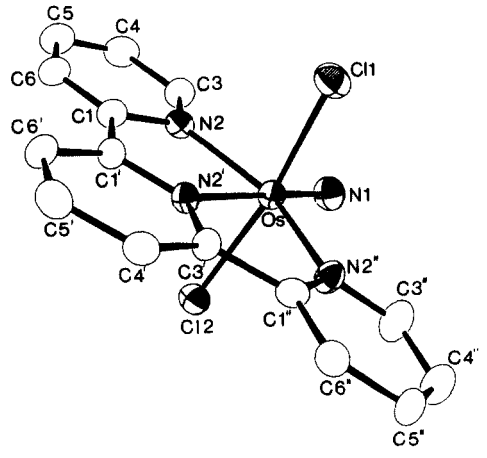

Figure 2. View of the $[Os(N)(tpy)(Cl)_2]^+$ cation in crystals of $[Os(N)(tpy)Cl_2]Cl$. Hydrogen atoms are omitted for clarity.

Table III. Bond Lengths (Å) in $[Os(N)(tpy)(Cl)_2]Cl$ as in Figure 1

atoms	distance	atoms	distance
Os-Cl(1)	2.348 (1)	C(1)-C(1')	1.473 (7)
Os-Cl(2)	2.344 (1)	C(3)-C(4)	1.379 (9)
Os-N(1)	1.663 (5)	C(4)-C(5)	1.354 (9)
Os-N(2)	2.073 (4)	C(5)-C(6)	1.380 (8)
Os-N(2')	2.162 (4)	C(1')-C(6')	1.403 (7)
Os-N(2'')	2.086 (4)	C(3')-C(4')	1.383 (7)
N(2)-C(1)	1.379 (6)	C(3')-C(1'')	1.468 (7)
N(2)-C(3)	1.332 (7)	C(4')-C(5')	1.370 (8)
N(2')-C(1')	1.331 (6)	C(5')-C(6')	1.374 (8)
N(2')-C(3')	1.342 (6)	C(1'')-C(6'')	1.362 (7)
N(2'')-C(1'')	1.380 (6)	C(3'')-C(4'')	1.360 (9)
N(2'')-C(3'')	1.330 (7)	C(4'')-C(5'')	1.361 (9)
C(1)-C(6)	1.380 (7)	C(5'')-C(6'')	1.368 (8)

and a view of the whole cation is presented in Figure 2. The bond lengths and angles in the cation are given in Tables III and IV, respectively.

The coordination around the osmium is approximately octahedral. The ligating atoms are two trans chlorides, three tpy nitrogen atoms, and the nitrido nitrogen atom. The distortions from idealized octahedral geometry are severe, the trans angles being 150.4 (2)°, 165.0 (5)°, and 179.6 (2)°. The constraints due to the chelation of the tpy ligand appear in the N(2)-Os-N(2'') angle of 150.4 (2)°. The Cl(1)-Os-Cl(2) angle of 165.0 (5)° is also bent considerably away from 180°. As is apparent in Figure 2, the bending is away from the nitrido ligand, N(1), and toward the tpy ligand. The distortion takes place entirely in the Os, N(1), Cl(1), Cl(2), N(2') plane. These five atoms remain coplanar in the complex. The Os-Cl distances of 2.344 (2) and 2.348 (2) Å are approximately equal and are comparable to values found in other six-coordinate complexes of Os(VI).[12]

The Os-N(1) bond length of 1.663 (5) Å for the nitrido ligand is relatively long. It does fall within the range of 1.570 (7) to 1.830 (4) Å reported for the other second- and third-row metal complexes containing a terminal nitrido ligand.[12-29] Terminal nitrido complexes of the first row exhibit shorter M-N bond lengths, which fall in the range of 1.512 (2) to 1.565 (6) Å.[30-32] Dehnicke and Strahle[27] have noted that, with only two exceptions, all second- and third-row M-N(nitrido) bond lengths fall in the range of 1.57-1.66 Å. This places the present complex at the upper end of this group. The M-N bond is longer than the values of 1.600 (11) Å in $[Os(N)(Cl)_4]^-$, 1.614 (13) Å in $[Os(N)(Cl)_5]^{2-}$, and 1.626 (17) Å in $[Os(N)(I)_4]^-$, all of which also contain Os(VI)-nitrido groups.[12,16,18]

Table IV. Bond Angles (deg) in $[Os(N)(tpy)(Cl)_2]Cl$ as in Figure 1

atoms	angle	atoms	angle
Cl(1)-Os-Cl(2)	165.05 (5)	N(2)-C(1)-C(6)	120.1 (5)
Cl(1)-Os-N(1)	97.6 (1)	N(2)-C(1)-C(1')	116.0 (4)
Cl(1)-Os-N(2)	89.5 (1)	C(6)-C(1)-C(1')	123.9 (5)
Cl(1)-O-N(2')	82.7 (1)		
Cl(1)-Os-N(2'')	88.5 (1)	N(2)-C(3)-C(4)	122.8 (6)
Cl(2)-Os-N(1)	97.4 (1)	C(3)-C(4)-C(5)	119.5 (6)
Cl(2)-Os-N(2)	86.6 (1)	C(4)-C(5)-C(6)	118.9 (6)
Cl(2)-Os-N(2')	82.3 (1)	C(1)-C(6)-C(5)	120.4 (6)
Cl(2)-Os-N(2'')	87.8 (1)		
N(1)-Os-N(2)	104.7 (2)	N(2')-C(1')-C(1)	112.9 (4)
N(1)-Os-N(2')	179.6 (2)	N(2')-C(1')-C(6')	119.1 (5)
N(1)-Os-N(2'')	104.8 (2)	C(1)-C(1')-C(6')	128.0 (5)
N(2)-Os-N(2')	75.6 (1)		
N(2)-Os-N(2'')	150.4 (1)	N(2')-C(3')-C(4')	118.9 (4)
N(2')-Os-N(2'')	74.9 (1)	N(2')-C(3')-C(1'')	112.6 (4)
		C(4')-C(3')-C(1'')	128.3 (5)
Os-N(2)-C(1)	117.4 (3)		
Os-N(2)-C(3)	124.3 (4)	C(3')-C(4')-C(5')	119.1 (5)
C(1)-N(2)-C(3)	118.3 (5)		
		C(4')-C(5')-C(6')	121.2 (5)
Os-N(2')-C(1')	118.0 (3)		
Os-N(2')-C(3')	118.5 (3)	C(1')-C(6')-C(5')	118.2 (5)
C(1')-N(2')-C(3')	123.4 (4)		
		N(2'')-C(1'')-C(3')	115.7 (4)
Os-N(2'')-C(1'')	118.0 (3)	N(2'')-C(1'')-C(6'')	119.9 (5)
Os-N(2'')-C(3'')	123.4 (4)	C(3')-C(1'')-C(6'')	124.3 (5)
C(1'')-N(2'')-C(3'')	118.6 (5)		
		N(2'')-C(3'')-C(4'')	122.8 (6)
		C(3'')-C(4'')-C(5'')	118.8 (6)
		C(4'')-C(5'')-C(6'')	119.8 (6)

Presumably, the steric requirements imposed by the tpy ligand are consistent with the suggestion made by Bright and Ibers that the M-N (nitrido) bond length is determined in large part by steric factors.[12] This would at least explain the elongation found for the tpy complex compared to $[Os(N)(Cl)_5]^{2-}$. In the present case, the combination of the observed Os-N(1) bond length of 1.663 (5) Å and the Cl(1)-Os-Cl(2) angle of 165.5 (5)° leads to N(1)-Cl(1) and N(1)-Cl(2) distances of 3.050 (5) and 3.043 (5) Å, respectively, which may be regarded as optimal.[12] The nitrogen atoms cis to the nitrido ligand [N(2) and N(2'')] also bend away from the nitrido group. The N(1)-Os-N(2) and N(1)-Os-N(2'') angles are 104.7 (2)° and 104.8 (2)°, respectively. While this effect is primarily due to the requirements of the tpy chelate "bite" angles, it does serve to accommodate further the nitrido ligand. In the present complex, as in other six-coordinate nitrido complexes, all four cis ligands are bent away from the nitrido group. This is an expected consequence of the multiple bond to Os. Multiple bonding along the Os-N bond axis leads to enhanced repulsive electronic interactions with the adjacent cis ligands.

As is usually the case,[27] the nitrido ligand exerts a strong trans effect in this complex. Thus, the Os-N(2') bond length of 2.162 (4) Å is significantly greater than the Os-N(2) and Os-N(2'') bonds of 2.073 (4) and 2.086 (4) Å, respectively. The discrepancy

(12) Bright, D.; Ibers, J. A. *Inorg. Chem.* **1969**, *8*, 709.
(13) Corfield, P. W. R.; Doedens, R. J.; Ibers, J. A. *Inorg. Chem.* **1967**, *6*, 197.
(14) Doedens, R. J.; Ibers, J. A. *Inorg. Chem.* **1967**, *6*, 204.
(15) Jaeger, F. M.; Zanstra, J. E. *Recl. Trav. Chim.* **1932**, *51*, 1013.
(16) Atovmyan, L. O.; Bokii, G. B. *Zh. Strikt. Khim.* **1960**, *1*, 501.
(17) Fletcher, S. R.; Griffith, W. P.; Pawson, D.; Phillips, F. L.; Skapski, A. C. *J. Cryst. Mol. Struct.* **1975**, *5*, 83.
(18) Fletcher, S. R.; Skapski, A. C.; Withers, M. *J. Trans. Met. Chem.* **1975**, *1*, 28.
(19) Phillips, F. L.; Skapski, A. C. *Acta Crystallogr. Sect. B* **1975**, *B31*, 2667.
(20) Hursthouse, M. B.; Motevalli, M. *J. Chem. Soc., Dalton Trans.* **1979**, 1362.
(21) Dehnicke, K.; Schmitte, J.; Fenske, D. *Z. Naturforsch.* **1980**, *B35*, 1070.
(22) Schweda, E.; Strahle, J. *Z. Naturforsch.* **1980**, 1146.
(23) Beck, J.; Schweda, E.; Strahle, J. *Z. Naturforsch.* **1985**, *B40*, 1073.
(24) Fenske, D.; Liebelt, W.; Dehnicke, K. *Z. Anorg. Allg. Chem.* **1980**, *467*, 83.
(25) Kropp, B.; Lorcher, K. P.; Strahle, J. *Z. Naturforsch.* **1977**, *B32*, 1361.
(26) Dehnicke, K.; Kruger, N.; Kujanek, R.; Weller, F. *Z. Kristallogr.* **1980**, *153*, 181.
(27) Dehnicke, K.; Strahle, J. *J. Angew. Chem.* **1981**, *93*, 451.
(28) Liese, W.; Dehnicke, K.; Rogers, R. D.; Shakir, R.; Atwood, J. L. *J. Chem. Soc., Dalton Trans.* **1981**, 1061.
(29) Hill, C. L.; Hollander, F. J. *J. Chem. Soc.* **1982**, *104*, 7318.

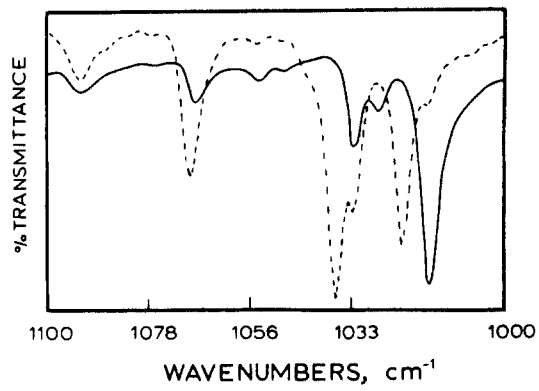

Figure 3. Infrared spectra of $[Os(N)(tpy)(Cl)_2]Cl$ (---) and its $[Os(^{15}N)(tpy)(Cl)_2]Cl$ analogue (—) in the $\nu(Os{\equiv}N)$ region in KBr pellets.

cannot be attributed to a stereochemical requirement of the tpy ligand. In two recently reported seven-coordinated tpy complexes of molybdenum, all Mo–N(tpy) distances were approximately equal.[23,24] The tpy ligand is not planar, but it can be viewed as consisting of three planar pyridine rings. The rings containing N(2) and N(2′) are approximately coplanar, the dihedral angle between them being only 3.3°. The rings containing N(2′) and N(2″) exist at a dihedral angle of 8.7° and the dihedral angle between the two outside rings is 9.4°. The distortion from planarity is much less than has been observed in other tpy complexes where dihedral angles in excess of 24° have been reported.[24,33]

The values of the eleven C–H bond lengths in the present structure are in the range of 0.79 (5) to 1.06 (5) Å, with an average of 0.89 (8) Å. The average value is comparable to the value of 0.95 Å normally associated with C–H distances obtained from X-ray structure determinations.[33]

Spectroscopic Properties and Solution Chemistry. Infrared studies have shown that a mode largely of $\nu(Os{\equiv}N)$ character is commonly observed in the region 1000–1120 cm^{-1} for nitrido complexes of Os(VI).[5,7c] In the infrared spectrum of $[Os(N)(bpy)(Cl)_3]$, $\nu(Os{\equiv}^{14}N)$ was observed at 1086 cm^{-1} as verified by the expected shift of 35 cm^{-1} to 1051 cm^{-1} upon ^{15}N labeling. The infrared spectra of ^{14}N and ^{15}N *trans*-$[Os(N)(tpy)(Cl)_2]Cl$ in KBr pellets are shown in Figure 3. The situation with regard to $\nu(Os{\equiv}N)$ is less clear in this cation. From comparisons with other tpy complexes, the band at 1033 cm^{-1} has its origin in the tpy ligand. The changes in band intensities and positions upon exchange of ^{15}N for ^{14}N suggest that the $\nu(Os{\equiv}N)$ mode may be mixed with other modes, making an unequivocal assignment of a "$\nu(Os{\equiv}N)$" mode ambiguous at best. The differences between the ^{14}N and ^{15}N spectra include the loss of bands at 1036 and 1020 cm^{-1} and the appearance of a band at 1016 cm^{-1} for the ^{15}N-labeled complex.

In the ^1H NMR spectrum of *trans*-$[Os^{VI}(N)(tpy)(Cl)_2]Cl$ measured in CD_3CN, a series of resonances appear that are characteristic of the coordinated tpy ligand.[34,35] There is no evidence in the spectrum for paramagnetic broadening or shifts of the resonances showing that the complex is diamagnetic.

In acetonitrile, the complexes *trans*-$[Os^{VI}(N)(tpy)(X)_2]^+$ (X = Cl^- or Br^-) appear to be stable over a period of several hours. Intra $d\pi \rightarrow d\pi$ transitions are expected for the d^2 configuration of Os(VI), but they are LaPorte forbidden and, therefore, expected to have relatively low molar extinction coefficients. Low-energy, weak ($\epsilon < 300\ M^{-1}\ cm^{-1}$) absorption bands do appear in the spectra in acetonitrile at λ_{max} = 530 nm (X = Cl) (insert, Figure 4) and at 550 nm (X = Br). The relatively low intensity of these bands points to $d\pi \rightarrow d\pi$ transitions as their origin.

Intense, high-energy bands ($\epsilon > 10^3\ M^{-1}\ cm^{-1}$) appear at λ_{max} = 354, 334, and 289 nm (X = Cl, Figure 4) and at 383 (sh), 342, 333 (sh), and 296 nm (X = Br). Related features appear in the spectra of $[N(n\text{-}Bu_4)][Os(N)(Cl)_4]$ and $[N(n\text{-}Pr_4)][Os(N)(Cl)_4(H_2O)]$.[36] A probable origin for at least some of these bands is in N → Os ligand-to-metal charge-transfer (LMCT) transitions.

The electronic absorption spectrum of the Os(III) ammino complex, $[Os(NH_3)(tpy)(Cl)_2](PF_6)$, measured in acetonitrile exhibits a weak band at 456 nm ($\epsilon \sim 10^3\ M^{-1}\ cm^{-1}$) and $\pi \rightarrow \pi^*$ absorption bands at 312 and 276 nm, respectively. The electronic absorption spectrum of this complex in 3 M HCl or water exhibits λ_{max} = 442, 306, 284, and 276 nm.

As shown in Figure 4, the spectrum of *trans*-$[Os^{VI}(N)(tpy)(Cl)_2]^+$ undergoes significant changes in acidic aqueous solution. Related changes occur in acetonitrile solution upon the addition of mineral acids. The chemistry, which appears to involve acid-catalyzed loss of chloride, is suppressed if Cl^- is added to the solution in excess of 1 M. Although the complex persists for several minutes at pH = 7, the loss of Cl^- is "instantaneous" at pH = 1. After loss of Cl^-, the absorption spectrum is unchanged over a period of hours. We have been unable to isolate and characterize satisfactorily the Cl^- loss product. It is a diprotonic acid. A potentiometric acid–base titration of *trans*-$[Os^{VI}(N)(tpy)(Cl)_2]^+$ after loss of Cl^- gave pK_{a_1} = 3.7 and pK_{a_2} = 5.5 at 298 K, μ = 0.1 M.

The complex *trans*-$[Os^{VI}(N)(tpy)(Cl)_2]^+$, or its hydrolysis product, is unstable over extended periods at pH > 7.0 as shown by spectrophotometric observations. The decomposition chemistry is accompanied by the appearance of characteristic $Os^{II} \rightarrow$ tpy metal-to-ligand charge-transfer absorption bands in the visible.[35] The gaseous product N_2O was also produced as shown by gas chromatography. We were unable to isolate the Os(II) product in pure form.

Electrochemistry. Cyclic voltammograms of *trans*-$[Os(N)(tpy)(Cl)_2]Cl$ and of $[Os(NH_3)(tpy)(Cl)_2]Cl$ in 3 M HCl (to suppress loss of Cl^-) are shown in Figure 5. For the ammino complex (Figure 5B) a wave for the Os(III)/(II) couple appears at −0.18 V and an additional oxidation wave at $E_{p,a}$ = 0.96 V before the onset of the background oxidation of Cl^-. The Os(III/II) wave is recovered after scan reversal past the wave at $E_{1/2}$ = 0.90 V. In a solution containing *trans*-$[Os(N)(tpy)(Cl)_2]Cl$, an initial reductive scan reveals a multielectron wave at $E_{p,a}$ = −0.19 V. Upon scan reversal, a new oxidative component appears for the $[Os(NH_3)(tpy)Cl_2]^{+/0}$ couple at $E_{p,a}$ = −0.14 V. Electrochemical reduction (at E_{app} = −0.3 V vs SSCE; n = 4 by coulometry) of *trans*-$[Os(N)(tpy)(Cl)_2]^+$ occurs quantitatively to give $[Os(NH_3)(tpy)Cl_2]^0$. The net reaction is shown below. The reduced product that was isolated and characterized was the PF_6^- salt of the Os(III) complex $[Os(NH_3)(tpy)(Cl)_2]^+$ formed by aerial oxidation of Os(II) upon workup.

$$trans\text{-}[Os^{VI}(N)(tpy)(Cl)_2]^+ + 4e^- + 3H^+ \rightarrow [Os(NH_3)(tpy)(Cl)_2]$$

Cyclic voltammograms of *trans*-$[Os^{VI}(N)(tpy)(Cl)_2]Cl$ and $[Os^{III}(NH_3)(tpy)(Cl)_2](PF_6)$ in acetonitrile are shown in Figure 6. For the ammino complex, a reductive wave appears at $E_{1/2}$ = −0.13 V for the Os(III)/(II) couple and an oxidative wave at $E_{1/2}$ = +1.19 V for an Os(IV)/(III) couple. The separation between $E_{1/2}$ values for the Os(IV)/(III) and the Os(III)/(II) couples is 1.26 V. This difference in potential is similar to that observed for the Os(IV)/(III) and Os(III)/(II) couples of $[Os(bpy)_2(Cl)_2]$ under the same conditions.[37] Electrochemical reduction of the nitrido complex, Figure 6A, gives rise to two new couples at $E_{p,a}$ = +0.32 V and $E_{1/2}$ = 1.39 V. The nature of the reduction product or products is currently under investigation.

(30) Buchler, J. W.; Dreher, C.; Lay, K.-L.; Lee, Y. J. A.; Scheidt, W. R. *Inorg. Chem.* **1983**, *22*, 888.
(31) Groves, J. T.; Takahashi, T.; Butler, W. M. *Inorg. Chem.* **1983**, *22*, 884.
(32) Beck, J.; Strahle, J. *Z. Naturforsch.* **1985**, *B40*, 891.
(33) Churchill, M. R. *Inorg. Chem.* **1973**, *12*, 1213.
(34) Lytle, F. E.; Petrosky, L. M.; Carlson, L. R. *Anal. Chim. Acta* **1971**, *57*, 239.
(35) Pipes, D. W.; Meyer, T. J. *J. Am. Chem. Soc.* **1984**, *106*, 7653.
(36) (a) Cowman, C. D.; Trogler, W. C.; Mann, K. R.; Poon, C. K.; Gray, H. *Inorg. Chem.* **1976**, *15*, 1747. (b) Constable, E. C. *J. Chem. Soc., Dalton Trans.* **1985**, 2687.
(37) Kober, E. M.; Caspar, J. V.; Sullivan, B. P.; Meyer, T. J. *Inorg. Chem.* **1988**, *25*, 4589.

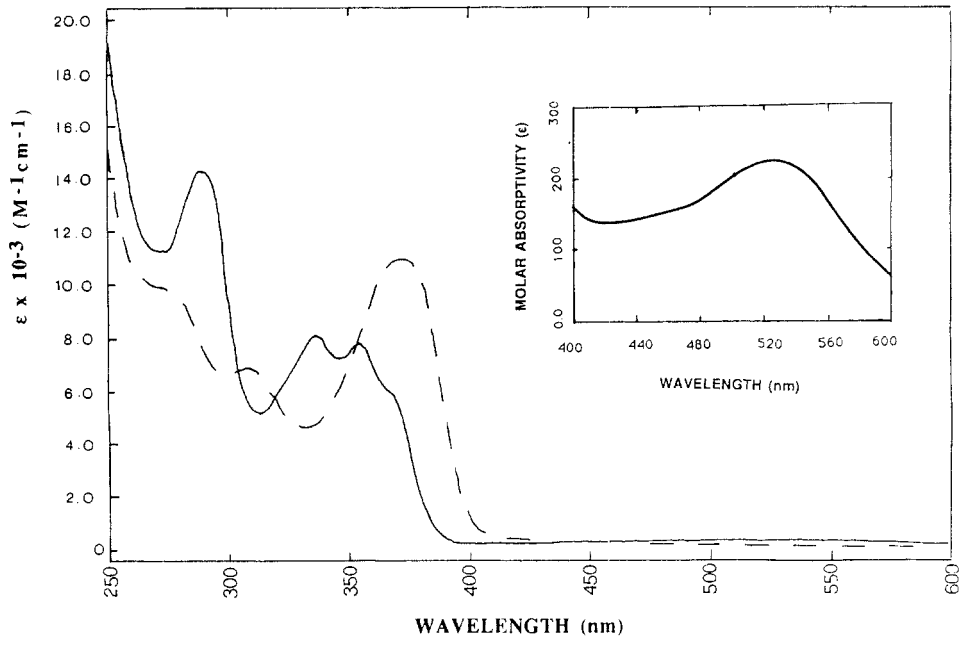

Figure 4. UV-vis spectra of $[Os(N)(tpy)(Cl)_2](PF_6)$ in CH_3CN solution (—) and in 0.1 M H_2SO_4 (---).

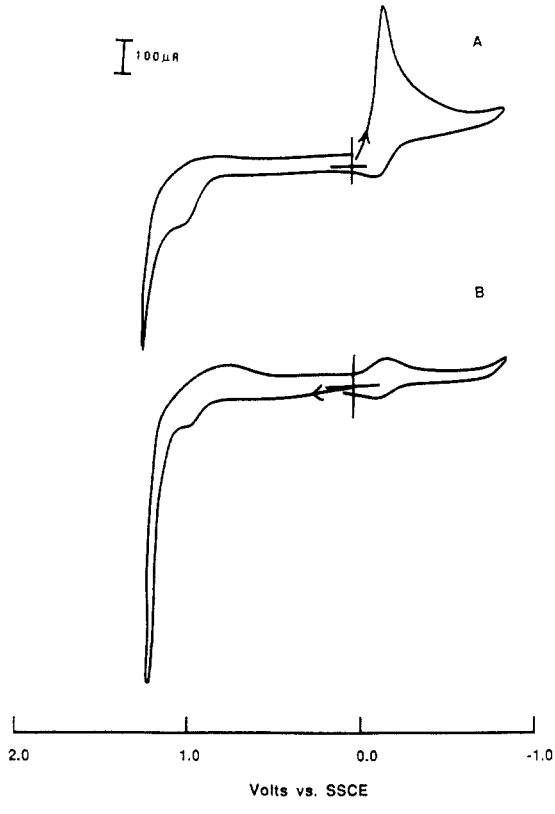

Figure 5. Cyclic voltammograms of (A) *trans*-$[Os(N)(tpy)(Cl_2)]Cl$ (10^{-2} M) and (B) $[Os(NH_3)(tpy)(Cl)_2]PF_6$ (10^{-2} M) in 3 M HCl. Glassy carbon disc working electrode (0.07 cm^2) at a scan rate of 200 mV/s vs SSCE.

The quasireversible wave at $E_{1/2}$ = 0.95 V arises from the $Cl_2/2Cl^-$ couple.

We have investigated the electrochemistry of $[Os(NH_3)(tpy)(Cl)_2]^+$ over an extended pH range, Figure 7. Cyclic voltammograms were obtained at pH = 1.2, 3.0, 5.5, 6.8, and 8.7. A detailed interpretation of the results is made difficult by the existence of kinetic effects and the pH dependences of the various couples. However, some insightful conclusions can be drawn from the data.

In aqueous solution at pH = 1.2 (0.1 M trifluoromethanesulfonic acid), two additional oxidative waves are observed past

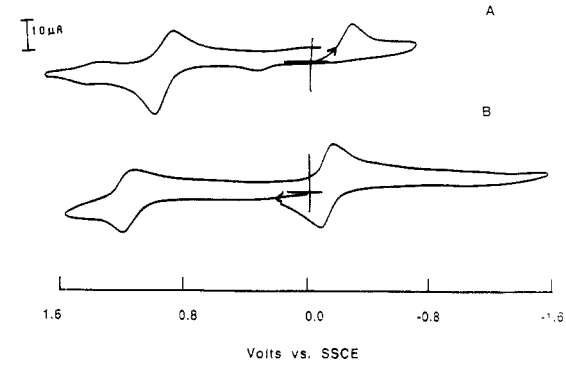

Figure 6. Cyclic voltammograms of (A) *trans*-$[Os(N)(tpy)(Cl)_2]Cl$ (10^{-3} M) and (B) $[Os(NH_3)(tpy)Cl_2]PF_6$ (10^{-3} M) in acetonitrile (0.1 M TBAH). Pt disc working electrode (0.125 cm^2) at a scan rate of 200 mV/s vs SSCE.

the Os(III)/(II) wave. The Os(IV)/(III) couple is quasireversible with $E_{1/2}$ = 0.85 V. If the scan is reversed before the further oxidation of Os(IV), it is chemically reversible on the time scale of the voltammetric scan. In acidic aqueous solution, the potentials for the Os(IV)/(III) and Os(III)/(II) couples are shifted reductively by −0.34 and −0.04 V compared to acetonitrile. The oxidation at $E_{p,a}$ = 1.13 V is both chemically and electrochemically irreversible. Scan reversal past this wave gave rise to a multielectron reduction wave whose potential was that anticipated for the reduction of *trans*-$[Os^{VI}(N)(tpy)(Cl)_2]^+$. At this pH, this wave overlaps with the reductive component of the $[Os(NH_3)(tpy)(Cl)_2]^{+/0}$ couple. From relative peak areas, oxidation past the Os(IV) stage appears to involve the loss of two electrons to give *trans*-$[Os^{VI}(N)(tpy)(Cl)_2]^+$. Loss of chloride appears to be triggered by oxidation past Os(IV) even on the cyclic voltammetric time scale. This is shown by the appearance of a small, pH-dependent wave at $E_{p,c}$ = 0.25 V on the return sweep, which may be attributed to the Os(III/II) couple of an aqua complex, possibly $[Os(NH_3)(tpy)(H_2O)Cl]^+$.

At pH = 3.0, the same pattern of waves was observed. However, the Os(VI) reduction wave shifts slightly as shown by the broadening on the low-potential side of the combined Os(VI)–Os(III) reduction wave, which appears at $E_{p,c}$ = −0.38 V.

From the data in acidic solution, a series of redox events exist. They lead to the interconversion between $Os^{II}(NH_3)^0$ and $Os^{VI}{\equiv}N^+$. The reactions suggested by the data are shown in Scheme I.

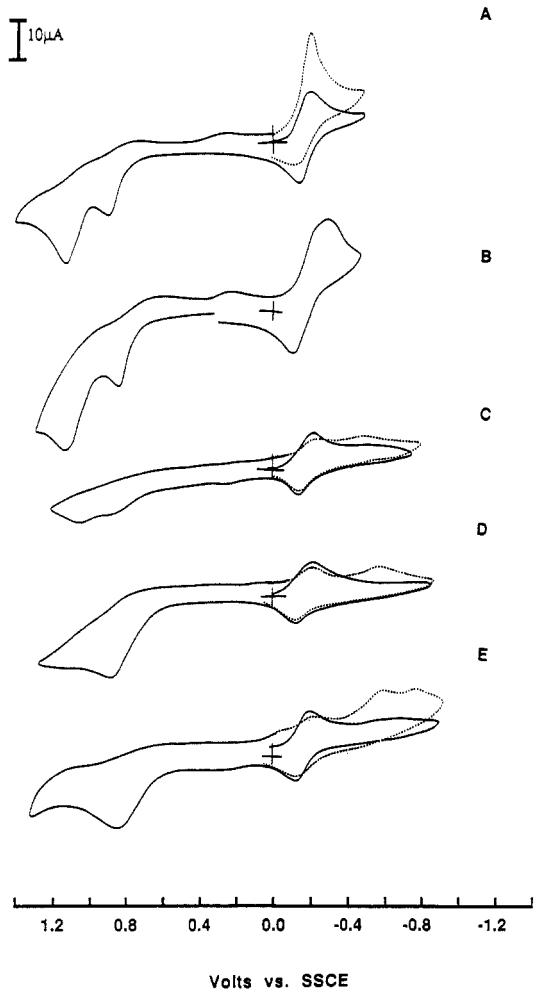

Figure 7. Cyclic voltammograms of $[Os^{III}(NH_3)(tpy)(Cl)_2]^+$ (10^{-2} M) at various pH values: (—) first scan and (···) second scan following the oxidative scan; (A) pH = 1.2, (B) pH = 3.0, (C) pH = 5.3, (D) pH = 6.8, and (E) pH = 8.7. Glassy carbon disc working electrode (0.07 cm^2) at a scan rate of 100 mV/s vs SSCE.

Scheme I

$$[Os^{II}(NH_3)(tpy)(Cl)_2] \underset{+e^-}{\overset{-e^-}{\rightleftharpoons}} [Os^{III}(NH_3)(tpy)Cl_2]^+$$

$$[Os^{III}(NH_3)(tpy)(Cl)_2]^+ \underset{+e^-}{\overset{-e^-}{\rightleftharpoons}} [Os^{IV}(NH_3)(tpy)(Cl)_2]^{2+}$$

$$[Os^{IV}(NH_3)(tpy)(Cl)_2]^{2+} \underset{+2e^-,\,+3H^+}{\overset{-2e^-,\,-3H^+}{\rightleftharpoons}} [Os^{VI}(N)(tpy)(Cl)_2]^{3+}$$

From Scheme I, oxidation past Os(IV) is a two-electron process that occurs without evidence for Os(V) as a stable, intermediate oxidation state. In the reduction of *trans*-$[Os^{VI}(N)(tpy)(Cl)_2]^+$, a multielectron wave appears at which Os(VI) is reduced to $[Os^{IV}(NH_3)(tpy)(Cl)_2]^{2+}$ and then the Os(IV) complex is reduced further to $[Os^{II}(NH_3)(tpy)(Cl)_2]$. The potentials for the Os(IV)/(III) and Os(III)/(II) couples must be the same or more positive than the potential for reduction of *trans*-$[Os^{VI}(N)(tpy)(Cl)_2]^+$ to Os(IV). The net reduction is a four-electron process.

$$trans\text{-}[Os^{VI}(N)(tpy)(Cl)_2]^+ + 4e^- + 3H^+ \rightarrow [Os^{II}(NH_3)(tpy)(Cl)_2]$$

One outcome of this analysis is that there is a very large peak-to-peak separation, $\Delta E_p \sim 1.48$ V, for the Os(VI)/(IV) couple at pH = 3.0. The extraordinary degree of electrochemical irreversibility exhibited by this couple is not surprising given the multiple electron/multiple proton requirements of the reaction.

Although Os(IV) is stable on the cyclic voltammetric time scale, it is thermodynamically unstable with regard to disproportionation, reaction 2. In a potential hold experiment, where the potential

$$3[Os^{IV}(NH_3)(tpy)(Cl)_2]^+ \rightarrow [Os^{VI}(N)(tpy)(Cl)_2]^+ + 2[Os^{III}(NH_3)(tpy)(Cl)_2]^+ + 3H^+ \quad (2)$$

was held just past the Os(IV)/(III) wave at $E_{p,a} = 0.90$ V, there was no evidence for a wave for the Os(IV)/Os(III) couple on the return scan. Rather, reduction waves for $Os^{III}(NH_3)^+$ and $Os^{VI}{\equiv}N^+$ were observed.

From the voltammogram at pH = 5.5 in Figure 7C, the Os(IV)/(III) couple and the reduction of $Os^{VI}{\equiv}N^+$ both exhibit pH effects. The peak currents were greatly diminished as the pH was increased. The $Os^{VI}{\equiv}N^+$ reduction wave appears at $E_{p,c} = -0.48$, well-separated from the pH-independent $Os^{III}NH_3^+/Os^{II}(NH_3)^0$ wave. Electrode kinetic effects appear to play an important role in giving less well defined electrochemical responses. The peak currents are diminished for all waves except the wave for the Os(III)/(II) couple. The $Os^{VI}{\equiv}N^+$ reduction remains multielectron in character. This is shown by the appearance of the oxidative component for the Os(III)/(II) couple on a reverse scan following reduction of $Os^{VI}{\equiv}N^+$.

The existence of pH and kinetic effects also complicates the voltammograms at pH = 6.8 and 8.7 (Figure 7, D and E). Compared to pH = 5.5, at pH = 6.8 there is a shift and a broadening of the $Os^{VI}{\equiv}N^+$ reduction at $E_{p,c} = -0.58$ V. By pH = 8.7, the broad wave has split into pH-independent and pH-dependent waves at $E_{p,c} = -0.58$ V and $E_{p,c} = -0.77$ V, respectively.

By pH = 6.8 the wave for the $Os^{IV}{-}NH_3^{2+}/Os^{III}{-}NH_3^+$ couple has been overtaken by the multielectron wave for the oxidation of $Os^{IV}{-}NH_3^{2+}$ to $Os^{VI}{\equiv}N^+$. As the pH is raised, deprotonated kinetic intermediates may speed up the rate and decrease the overvoltage for the oxidation of $Os^{IV}{-}NH_3^{2+}$. It has been suggested that the deprotonated intermediates $[M^{III}(NH_2)(tpy)(bpy)]^{2+}$ (M = Ru or Os) play a role in the oxidation of coordinated ammonia to nitrosyl.[2] The effects of deprotonation come past the reversible Os(IV)/(III) couple, at the Os(IV) → Os(VI) stage. This is consistent with the expected acidity of the Os(IV) ammine protons and the proton loss requirements of the net oxidation.[38] Proton loss and oxidation may occur via intermediates such as $[Os(NH_2)(tpy)(Cl)_2]^+$ or even $[Os(NH)(tpy)(Cl)_2]$. In a somewhat related chemistry, it has been reported that above pH = 4.0, the complex $[Ru^{III}(NH_3)(tpy)(bpy)]^{3+}$ undergoes a disproportionation to give $[Ru^{IV}(NH)(tpy)(bpy)]^{3+}$ and $[Ru^{II}(NH_3)(tpy)(bpy)]^{2+}$.[4] The effect of deprotonation is to enhance rates of oxidation at the electrode past the Os(IV) stage. The thermodynamic potentials for the higher oxidation stage Os(VI/V) and Os(V/IV) couples must be less oxidizing than the Os(IV/III) couple, see below. By pH = 6.8 the rates of oxidation of Os(IV) and Os(V) at the electrode are sufficiently rapid that only a single multielectron oxidation wave is observed. This wave arises from the oxidation of Os(III) to Os(VI), reaction 3.

$$[Os^{III}(NH_3)(tpy)(Cl)_2]^+ \xrightarrow{-3e^-,\,-3H^+} trans\text{-}[Os^{VI}(N)(tpy)(Cl)_2]^+ \quad (3)$$

Changes in pH also play a role reductively in the range pH = 6.8 to 8.7. By pH = 6.8 the $Os^{VI}{\equiv}N^+$ wave is split into two waves at $E_{p,a} = -0.58$ V and $E_{p,a} = -0.77$ V. From this behavior it can be inferred that the wave at −0.58 V arises from a pH-dependent, irreversible Os(VI)/(V) couple.

$$trans\text{-}[Os^{VI}(N)(tpy)(Cl)_2]^+ \xrightarrow{+e^-} [Os^{V}(N)(tpy)(Cl)_2]$$

The initial reduction of Os(VI) to Os(V) is followed by a second, pH-dependent reduction of Os(V) to Os(III) followed by further one-electron reduction of Os(III) to Os(II).

$$[Os^{V}(N)(tpy)(Cl)_2] \xrightarrow{+2e^-,\,+3H^+} [Os^{III}(NH_3)(tpy)(Cl)_2]^+$$

(38) Buhr, J. D.; Winkler, J. R.; Taube, H. *Inorg. Chem.* **1980**, *19*, 2416.

Scheme II

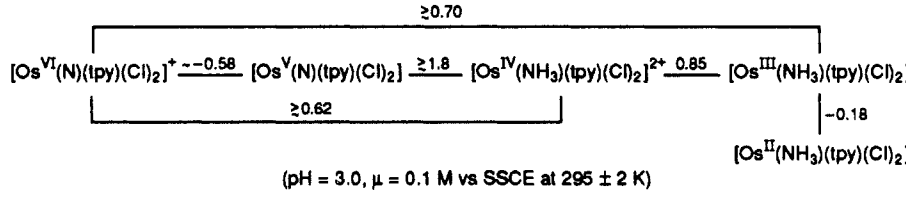

Discussion

The results presented here demonstrate that *trans*-$[Os(N)(tpy)(Cl)_2]^+$ and $[Os(NH_3)(tpy)(Cl)_2]$ can be reversibly interconverted by $4e^-/3H^+$ redox processes in acidic solution. The multiple electron transfer chemistry is reminiscent of the reversible $6e^-/5H^+$ interconversion that occurs between nitrosyl and ammonia in related polypyridyl complexes of Os and Ru, reaction 1.

The oxidation of $[Os(NH_3)(tpy)(Cl)_2]$ to *trans*-$[Os(N)(tpy)(Cl)_2]$ occurs via the intermediate oxidation states Os(III) and Os(IV). This redox chemistry is reminiscent of that of related aqua complexes of Ru and Os.[39] In both cases, oxidation occurs with a concomitant loss of electrons and protons. The reactions are driven by the stabilization of higher oxidation states through metal–oxo or metal–nitrido bond formation.

$$cis,trans\text{-}[Os(bpy)_2(H_2O)_2]^{2+} \rightarrow cis,trans\text{-}[Os(O)_2(bpy)_2]^{2+} \quad (4)^{39b}$$

In the nitrido complex, stabilization of oxidation state (VI) arises from a single Os–nitrido interaction and multiple Os–N bonding. The loss of protons upon oxidation frees $p\pi$ electron density for donation to the metal. Defining the *z* axis to lie along the Os–N bond, electron donation from appropriate linear combinations of the $2p_N$ nitrido orbitals to the d_{xz} and d_{yz} orbitals at the metal provides a basis for two π-bonding interactions. Mixing between the filled $2p_N$ and the two $d\pi$ orbitals imparts a considerable degree of antibonding character to d_{xz} and d_{yz}. This results in the relative energy ordering $d_{xy} < d_{xz}, d_{yz}$. This ordering accounts for the diamagnetism in the ground state of the d^2 Os(VI) complexes, which was shown by the absence of paramagnetic shifts in ^1H NMR spectra. It also provides an orbital basis for the appearance of the $d\pi \rightarrow d\pi$ transitions in the visible region of the spectrum.

In an electronic sense, nitrido bonding to Os(VI) in $[Os^{VI}(N)(tpy)(Cl)_2]^+$ is related to dioxo bonding to Os^{VI} in *trans*-$[Os(O)_2(bpy)_2]^{2+}$.[39b] The *trans*-dioxo complex is also a diamagnetic, d^2 ion. Defining the *z* axis to lie along the *trans*-dioxo bonding axis, the diamagnetism arises due to the extensive mixing between d_{xz}, d_{yz} and the $p\pi$ orbitals of the *trans*-O atoms. The resulting electronic configuration of the ground state is $(d_{xy})^2(d_{xz})^0(d_{yz})^0$.[39b]

The effects of multiple Os–N bonding by nitrido to Os(VI) donation appear in the crystal structure. The most direct consequence is the short Os–N bond length of 1.663 (5) Å. The repulsive effect of the electron density at the Os≡N bond appears in (1) the bending of the cis atoms away from the nitrido group and (2) the elongation of 0.08 Å of the trans N atom of the tpy ligand.

The Redox Couples that Interrelate Os(VI) and Os(II). In water, from pH = 1.2 to 5.5, the Os(III/II) and Os(IV/III) couples are pH independent and quasireversible electrochemically. Their potentials are consistent with what is to be expected for a relatively electron-rich, polypyridyl coordination environment around Os(II).[39c]

In the interconversion between oxidation states Os(III) and Os(VI), reaction 3, there are some features shared in common with the oxidation of $[Os^{III}(OH)(H_2O)(bpy)_2]^{2+}$ to *trans*-$[Os^{VI}(O)_2(bpy)_2]^{2+}$.

$$trans\text{-}[Os^{III}(OH)(H_2O)(bpy)_2]^{2+} \underset{+3e^-,\,+3H^+}{\overset{-3e^-,\,-3H^+}{\rightleftharpoons}} trans\text{-}[Os^{VI}(O)_2(bpy)_2]^{2+}$$

For *trans*-$[Os^{III}(OH)(H_2O)(bpy)_2]^{2+}$, only the three-electron Os(VI)/(III) couple, *trans*-$[Os^{VI}(O)_2(bpy)_2]^{2+}$/*trans*-$[Os^{III}(OH)(H_2O)(bpy)_2]^{2+}$, is accessible thermodynamically in acidic solution. In this coordination environment, oxidation states Os(V) and Os(IV) are stronger oxidants than Os(VI) and are unstable with respect to disproportionation into Os(VI) and Os(III).

In the oxidation of $[Os^{III}(NH_3)(tpy)(Cl)_2]^+$ to $[Os(N)(tpy)(Cl)_2]^+$, Os(IV) does appear in acidic solution or in acetonitrile. However, in water it is a kinetic intermediate that is unstable with respect to disproportionation, reaction 2. By pH = 6.8, where deprotonated forms enhance rates of oxidation–reduction at the electrode, only a single wave for the $3e^-$ oxidation of Os(III) to Os(VI) is observed in the voltammogram in Figure 7D. At this pH, Os(IV) is no longer observable even as a kinetic intermediate. For either the nitrido or *trans*-dioxo cases an important factor leading to the instability of the intermediate oxidation states is the electronic stabilization of the d^2 Os(VI) form by *trans*-dioxo or nitrido bonding.

The kinetically slow step in the interconversion between $Os^{III}(NH_3)^+$ and $Os^{VI}\equiv N^+$ is at the Os(IV) → Os(V) stage. It is at this stage that there is a significant change in proton content between adjacent oxidation states. From the appearance of the pH-independent reduction wave for *trans*-$[Os^{VI}(N)(tpy)(Cl)_2]^+$ at −0.58 V at pH = 8.7, the Os(VI/V) couple is pH independent, at least at this pH. This means that the interconversion between Os(IV) and Os(V) involves a loss of three protons and the couple $[Os^{V}(N)(tpy)(Cl)_2]^0/[Os^{IV}(NH_3)(tpy)(Cl)_2]^{2+}$.

Although the Os(VI)/(IV) couple is highly irreversible in an electrochemical sense, it is possible to obtain a crude estimate of its thermodynamic potential from the electrochemical data. Slow electrode kinetics at the Os(IV) → Os(V) stage shift the oxidative peak potential for the $Os^{VI}\equiv N^+/Os^{IV}(NH_3)^{2+}$ couple to potentials that are far more oxidative than the true potential for the couple. On the reductive side, the wave shape and peak positions are distorted by slow kinetics due to the proton loss requirements at the Os(V)/(IV) stage. There is the additional complication that the slow Os(V) to Os(IV) reduction must be preceded by the reduction of $Os^{VI}\equiv N^+$. Since that reduction occurs at −0.58 V, the concentration of $Os^{V}\equiv N^0$ is relatively low at the more positive peak potential for the Os(VI/IV) couple. From this analysis the difference in peak potentials for the multielectron oxidation and reduction waves, $(E_{p,a} - E_{p,c})/2 = 0.62$ V, should give a *lower* limit for the potential of the Os(VI/V) couple.

The pH-independent Os(VI/V) wave is chemically irreversible. If it is assumed that electron transfer is rapid and followed by a rapid chemical step, the peak potential, minus −0.03 V, provides an estimate for the potential of the Os(VI/V) couple.

The measured or estimated potentials for the series of couples at pH = 3 are collected in the Latimer diagram in Scheme II. These potentials provide a quantitative or, at least, semiquantitative basis for addressing some of the observations made concerning the descriptive chemistry of the nitrido/ammine system.

The low value of the potential for the Os(VI)/(V) couple shows the profound effect of the change in electron content between d^2 Os(VI) and d^3 Os(V). In this couple an electron is added to the antibonding d_{xz}, d_{yz} orbitals in oxidation state V. This has the

(39) (a) Gilbert, J. A.; Eggleston, D. S.; Murphy, W. R., Jr.; Geselowitz, D. A.; Gersten, S. W.; Hodgson, D. J.; Meyer, T. J. *J. Am. Chem. Soc.* **1985**, *107*, 3855. (b) Dobson, J. C.; Takeuchi, K. J.; Pipes, D. W.; Geselowitz, D. A.; Meyer, T. J. *Inorg. Chem.* **1986**, *25*, 2357. (c) Pipes, D. W.; Meyer, T. J. *Inorg. Chem.* **1986**, *25*, 4042. (d) Dobson, J. C.; Meyer, T. J. *Inorg. Chem.* **1988**, *27*, 3283.

Scheme III[a]

nominal electron count at the metal	dominant form of the complex	
$(d\pi)^6$	$[Os^{II}(NH_3)(tpy)(bpy)]^{2+}$	$[Os^{II}(NH_3)(tpy)(Cl)_2]^0$
$(d\pi)^5$	$[Os^{III}(NH_3)(tpy)(bpy)]^{3+}$	$[Os^{III}(NH_3)(tpy)(Cl)_2]^+$
$(d\pi)^4$	$[Os^{IV}(NH)(tpy)(bpy)]^{2+}$	$[Os^{IV}(NH_3)(tpy)(Cl)_2]^{2+}$
$(d\pi)^3$	$[Os^{V}(N)(tpy)(bpy)]^{2+}$ or $[Os^{II}(NH_2O)(tpy)(bpy)]$	$[Os^{V}(N)(tpy)(Cl)_2]$
$(d\pi)^2$/or $(d\pi)^6(\pi^*(NO))^2$	$[Os^{II}(NHO)(tpy)(bpy)]^{2+}$	$[Os^{VI}(N)(tpy)(Cl)_2]^+$
$(d\pi)^6(\pi^*[NO])^1$	$[Os^{II}(NO^*)(tpy)(bpy)]^{2+}$	
$(d\pi)^6$	$[Os^{II}(NO)(tpy)(bpy)]^{3+}$	

[a] pH = 3.0 vs SSCE.

effect of greatly diminishing the 1-electron oxidizing strength of $[Os(N)(tpy)(Cl)_2]^+$ even though the metal is in a high formal oxidation state. The potential for the related dioxo Os(VI)/(V) couple *trans*-$[Os(O)_2(bpy)_2]^{2+/+}$ (+0.21 V)[39b] is more positive by 0.8 V. This suggests that the multiple-bond interaction between N and Os(VI) in *trans*-$[Os(N)(tpy)(Cl)_2]^+$ may be considerably greater than that between the two oxo groups and Os(VI) in the electronically equivalent *trans*-dioxo complex. For the $3e^-/3H^+$ couples, *trans*-$[Os^{VI}(N)(tpy)(Cl)_2]^+$/*trans*-$[Os^{III}(NH_3)(tpy)(Cl)_2]^+$ and *trans*-$[Os^{VI}(O)_2(bpy)_2]^{+2}$/*trans*-$[Os^{III}(OH)(H_2O)(bpy)_2]^{+2}$,[39b] the potentials are >0.70 and 0.36 V at pH = 1.0.

The stabilization of Os(VI) is also the cause of the thermodynamic instability of Os(V) and Os(IV). Disproportionation of Os(IV), reaction 2, is favored by ≳0.2 V. Disproportionation of Os(V), reaction 5, is favored by >2.4 V.

$$3[Os^{V}(N)(tpy)(Cl)_2] + 3H^+ \rightarrow [Os^{III}(NH_3)(tpy)(Cl)_2]^+ + 2[Os^{VI}(N)(tpy)(Cl)_2]^+ \quad (5)$$

In aqueous acidic solution, Os(V) is both a strong reducing agent and a powerful oxidizing agent. It is highly unstable toward disproportionation.

The change in proton composition between oxidation states IV and V is expected to play a major role in the redox chemistry of this couple. Mechanisms that involve simple electron transfer and either reduction of Os(V) to give $[Os^{IV}(N)(tpy)(Cl)_2]^-$ or oxidation of Os(IV) to give $[Os^{V}(NH_3)(tpy)(Cl)_2]^{3+}$ necessarily occur via intermediates that are highly energetic with regard to proton content. It is this feature that causes the slowness of the couple at the electrode.[40]

Nitrido to Ammino Interconversion. Comparisons with Nitrosyl to Ammine Interconversion. In $[Os^{II}(NH_3)(tpy)(bpy)]^{2+}$ the coordination sphere at Os is closely related to that at $[Os^{II}(NH_3)(tpy)(Cl)_2]$ with the trans chloro groups replaced by a single bpy. The change in ligand composition and/or stereochemistry is sufficient to change the course of the oxidation chemistry in a significant way. The stepwise natures of the two oxidations, as deduced largely by electrochemical measurements, are shown in Scheme III. An organizing feature in the scheme is the inclusion of the electron content at the metal at each stage of the oxidation. For $[Os(NO)(tpy)(bpy)]^{3+}$ the scheme has been simplified by not considering competitive N–N coupling reactions that occur at the two-electron reduction stage to give nitrous oxide and at the three-electron stage to give N_2.[2]

The differences in behavior can be explained qualitatively. The exchange of chloride ions in $[Os^{II}(NH_3)(tpy)(Cl)_2]$ for bipyridine in $[Os^{II}(NH_3)(tpy)(bpy)]^{2+}$ removes electron density from the metal, making it more electron deficient. A measure of the effect is available by comparing reduction potentials. For the couples $[Os(NH_3)(tpy)(bpy)]^{3+/2+}$ and $[Os(NH_3)(tpy)Cl_2]^{+/0}$, the potentials are −0.43 and −0.18 V at 22 ± 2 °C, μ = 0.1 M in H_2O vs. SSCE. For the corresponding Os(IV)/(III) couples, the values of the potential are >1.8 V for $[Os(NH_3)(tpy)(bpy)]^{4+/3+}$ and 0.85 V for $[Os(NH_3)(tpy)Cl_2]^{2+/+}$.

In the more electron rich coordination environment of the dichloro complex, Os(IV) is accessible at a reasonable potential by simple oxidation although it is thermodynamically unstable with regard to disproportionation. Access to Os(IV) in the tpy–bpy coordination environment at accessible potentials requires proton loss and π donation from the nitrogen atom to give an imido complex.

A major divergence in behavior occurs at the $4e^-$ oxidation stage. The results of proton-dependent electrochemical studies suggest that in the absence of N–N coupling the bpy complex would exist as $[Os^{II}(NHO)(tpy)(bpy)]^{2+}$ at this stage. The dichloro complex exists as *trans*-$[Os^{VI}(N)(tpy)(Cl)_2]^+$. The different forms have the same electron content and are related as conjugate acid–base pairs

$$[Os^{VI}(N)(tpy)(Cl)_2]^+ + H_2O \rightarrow [Os^{II}(NHO)(tpy)(Cl)_2] + H^+$$

The hydration step is an alternative to proton loss and π-donation as a means of stabilizing higher oxidation states. The addition of a base at the nitrogen atom causes the release of electron density to the metal.

In more basic solution, loss of an additional proton would lead

$$[Os^{II}(NHO)(tpy)(Cl)_2] + OH^- \rightarrow [Os^{II}(NO)(tpy)(Cl)_2]^- + H_2O$$

to the analogue of the twice-reduced nitrosyl, $[Ru(NO)(tpy)(bpy)]^+$, which has been observed electrochemically.[2] The probable existence of the acid–base chemistry for the dichloro complex can be inferred by the instability of *trans*-$[Os(N)(tpy)(Cl)_2]^+$ in basic solution. In the decomposition chemistry, N_2O is formed as a product. The electrochemical reduction of $[Os(NO)(tpy)(bpy)]^{3+}$ in water also gives N_2O apparently via the intermediate formation of a N–N coupled dimer.[3] In either case, the appearance of N_2O may be a product of $M^{II}(NHO)$ coupling.

Acknowledgements are made to the National Institutes of Health under Grant 5-R01-GM32296-07 for support of this research and to Professor Henry Taube for some very helpful comments concerning this work and for providing a copy of David Ware's dissertation.

Supplementary Material Available: Tables of H-atom parameters and anisotropic thermal parameters (2 pages); listing of calculated and observed F values for $[Os(N)(tpy)(Cl)_2]Cl$ (18 pages). Ordering information is given on any current masthead page.

(40) (a) Cabanis, G. E.; Diamantis, A. A.; Murphy, W. R., Jr.; Linton, W.; Meyer, T. J. *J. Am. Chem. Soc.* **1985**, *107*, 1845. (b) Binstead, R. A.; Meyer, T. J. *J. Am. Chem. Soc.* **1987**, *109*, 3287.